

Phytosynthesis, Antimicrobial and Catalytic Activities of Silver Nanoparticles Derived Using Leaf and Stem Extracts of *Indigofera macrophylla*

O. E. THOMAS^{*A-F}; †O. A. ADEGOKE^{A,B}; E. M. ADENIYI^{C-F}; C. G. OLIVER^{C-F}

Department of Pharmaceutical Chemistry, University of Ibadan, Ibadan 200284, Nigeria

†Deceased January 2021

A – research concept and design; B – collection and/or assembly of data; C – data analysis and interpretation; D – writing the article; E – critical revision of the article; F – final approval of article.

Abstract

Background: The phytosynthesis of metal nanoparticles is a promising green alternative to traditional chemical approaches.

Objective: The aim of this study was to synthesize silver nanoparticles (AgNPs) with antimicrobial and biocatalytic activities using aqueous leaf and stem extracts of *Indigofera macrophylla*.

Methods: Critical reaction variables for the biosynthesis of AgNPs were optimized using UV-vis spectroscopy before the biosynthesized AgNPs were characterized using various spectroscopic and microscopic techniques. The biological activities of the biogenic nanoparticles were then investigated with particular focus on their antimicrobial activity and biocatalytic efficiency in the degradation of methylene blue.

Results: The surface plasmon resonance of silver nanoparticles biosynthesized using aqueous extracts of leaf (LE-AgNPs) and stem (SE-AgNPs) of *I. macrophylla* occurred at 430 and 426 nm respectively. Scanning electron microscopy images of the nanoparticles showed highly aggregated polymorphs with mostly spherical shape. The particle sizes of LE-AgNPs and SE-AgNPs as determined by Transmission electron microscopy were 48.61 ± 8.60 and 18.09 ± 4.13 nm respectively with Energy dispersive X-ray analysis confirming characteristic absorption band at 3 KeV. In susceptibility assays, LE-AgNPs showed dose-dependent zones of inhibition against *Escherichia coli* (18 mm), *Staphylococcus aureus* (18 mm), *Pseudomonas aeruginosa* (20 mm) while SE-AgNP was only active against *Staphylococcus aureus* (10 mm). Both LE-AgNPs and SE-AgNPs showed good biocatalytic efficiency in the degradation of methylene blue with rate constants of 0.0204 and 0.0182 min^{-1} respectively.

Conclusion: Silver nanoparticles with antimicrobial and catalytic activities have been biosynthesized using the aqueous extract of *Indigofera macrophylla*.

Keywords: Silver nanoparticles, Methylene blue, Catalytic activity, Antimicrobial activity, *Indigofera macrophylla*

INTRODUCTION

Nanotechnology is a rapidly growing research field which deals with the fabrication, design and manipulation of nanomaterials with at least one dimension of the order of 1-100 nm (Rafique et al. 2017). The novel mechanical, optical, electronic and magnetic properties exhibited by nanomaterials compared to the bulk have stimulated interest in nanomaterials since their discovery. These unique

properties arise from the significant increase in surface-to-volume ratio as the particle downsizes to the nanoscale (Yusuf et al. 2020).

Among the variety of metal nanoparticles, colloidal silver possesses remarkable conductivity, chemical stability, catalytic and antibacterial activities (Rafique et al. 2017). Silver nanoparticles (AgNPs) have found applications as broad-spectrum antimicrobial coating

on medical devices as well as in degradation of organic dyes in effluent discharges of industries (Sharma et al. 2015; Al-Zaban et al. 2021). The aromatic stability of organic dyes, which are extensively used in printing, textile and drug industries, necessitates prolonged and expensive treatment processes before they can be safely discharged into water bodies. Conventional treatment methods including flocculation, sludge biochemical processes, electroanalytical degradation and reverse osmosis have been successfully employed but they remain expensive and potential sources of secondary pollution because of the use of chemicals to destroy the aromatic structure of the dyes (Sharma et al. 2015). Silver nanoparticles, which can act as biocatalyst that lower the activation energy required for the breakdown of the aromatic stability of organic dyes have therefore been employed as an inexpensive, eco-friendly and efficient method for their safe disposal (Fierascu et al. 2019; Al-Zaban et al. 2021). In addition, the antimicrobial activity of AgNPs can be employed in the safe removal of pathological bacteria from water bodies without some of the less desirable adverse impacts of conventional processes such as chlorine treatment (Menon et al. 2021).

Silver nanoparticles can be readily synthesized by the chemical reduction of silver ions. Alternatively, reduction can be achieved by biological methods including the use of microorganisms and plants extracts (Rafique et al. 2017). The green synthesis of AgNPs is efficient, inexpensive and eco-friendly. In addition, the use of plants extracts for biosynthesis offers the additional advantage of synthesizing

nanoparticles that are stabilized and capped by the plants' metabolites. Thus, nanoparticles with predefined characteristics can be synthesized using plants with the desired biological or (bio)chemical activities (Hemlata et al. 2020). For example, silver nanoparticles with bioactivities including antimicrobial, antiproliferative and catalytic activities have been synthesized using *Garcinia kola*, *Cucumis prophetarum* and *Ficus panda* extracts respectively (Tripathi et al. 2013; Labulo et al. 2016; Hemlata et al. 2020).

Indigofera macrophylla Schumach. & Thonn. (Family Fabaceae) is a climbing shrub that can reach 2-10 metres high (Adegoke and Ayodele 2017). The plant, which is indigenous to tropical West Africa, has pinnate-compound leaves with purple or red flowers (Nwankwo and Ayodele 2017). Traditionally, the leaves and stem of the plants are used in the treatment of a range of ailments including amoebic diarrhea, dysentery and whooping cough (Adegoke and Ayodele 2017). The leaf and stem extracts of *I. macrophylla* also possess chemosensing ability, a property we hypothesize can enhance the redox catalytic efficiency of AgNPs biosynthesized with the plant (Adegoke and Ayodele 2017).

The objective of this study was therefore to synthesize AgNPs with antimicrobial and catalytic activities using the aqueous extract of the leaves and stem of *Indigofera macrophylla*.

METHODOLOGY

Materials

Fresh *Indigofera macrophylla* plants were collected during the rainy season along Eruwa road, Ido local government area of Ibadan and voucher specimen (FHI number- 113019) were deposited at the Forestry Research Institute of Nigeria. Silver nitrate, ethanol, sodium borohydride were BDH (UK) products while Sabouraud dextrose agar and nutrient agar were sourced from Titan Biotech, India.

Preparation of plant extract

Heat-assisted aqueous extraction of the plant materials as described by other studies was employed (Hemlata et al. 2020; Oluwaniyi et al. 2016). Whole plants of *I. macrophylla* were first thoroughly washed under running tap water and then with distilled water. The leaf extract was prepared by weighing and cutting into small pieces 40 g of the leaves before the addition of

400 mL distilled water. The mixture was then heated at 60°C for 30 mins after which it was filtered using Whatmann filter No. 1 filter paper. The stem extract was similarly prepared with 40 g of the stem parts of the plant. The aqueous leaf and stem extracts were stored at 4°C until required for use.

Phytochemical screening

Using standard procedures followed by Hemlata et al. 2020, the leaf and stem extract of *I. macrophylla* were screened for the presence of bioactive compounds such as alkaloids, tannins, phenols, saponins, anthraquinones, flavonoids, terpenoids, steroids and cardiac glycosides.

Biosynthesis of silver nanoparticles

Method of Biosynthesis

The optimized procedure involved the addition of 10 mL of the leaf extract to 90 mL of 1 mM AgNO₃. The resulting solution was continuously stirred at room temperature for 8 hours. The reaction mixture was wrapped in aluminum foil to avoid photodegradation of AgNO₃ solution and the bioreduction of the solution was monitored by the colour change from light green to dark brown. Aliquots of the reaction mixture were taken at regular intervals for UV-visible data acquisition. A ratio of 20 mL extract to 80 mL 1mM AgNO₃ was found optimal for biosynthesis using the stem extract. The biosynthesized AgNPs were purified by first centrifuging at 15,000 rpm for 5 min before three cycles of washing with distilled water.

Optimization of reaction variables

The optimal concentration of silver nitrate was determined by adding fixed volumes of 1, 2, 3, 4, 5 and 6 mM solutions of silver nitrate to an equal volume of the extracts and monitoring the surface plasmon resonance characteristics of the AgNPs in each case. Optimal ratio of the volumes of silver nitrate solution and plant extracts were determined using the Job's method of stoichiometric ratio in which 0.1, 0.2, 0.3, 0.4, 0.5, 0.6, 0.7, 0.8 0.9 and 1.0 mL of the leaf and stem extracts were made up to 1 mL with 1 mM silver nitrate solution (Renny et al. 2013). The UV-vis spectrum of each of the reaction mixtures was then determined.

Characterization of biosynthesized AgNPs

The UV-vis spectral analysis of the nanoparticles biosynthesized using aqueous extracts of leaf (LE-AgNPs) and stem (SE-AgNPs) of *I. macrophylla* were acquired using a Cecil CE 2021 scanning UV-Vis spectrophotometer. The secondary metabolites present as capping and stabilizing agents on the AgNPs were determined using Nicolet iS10 FT-IR spectrometer. The particle size and distribution was determined using Transmission Electron Microscope (NanoMill 1040 model) while the elemental composition of the AgNPs were analysed using scanning electron microscope integrated with energy dispersive X-ray analysis.

Antimicrobial activity of LE-AgNPs and SE-AgNPs

Susceptibility assay

The antimicrobial activity of the LE-AgNPs and SE-AgNPs were screened against standard strains of microorganisms-*Staphylococcus aureus* ATCC 29213, *Escherichia coli* ATCC 25922, *Pseudomonas aeruginosa* ATCC 27853, *Bacillus subtilis*, *Trichophyton rubrum* and *Candida albicans* using the agar diffusion method. Bacteria were seeded into molten nutrient agar using the pour plate method while surface spreading on Sabouraud dextrose agar was used for fungi. Gentamicin and ketoconazole were employed as controls for bacteria and fungi respectively. Into each of the 8 mm wells in prepared agar plates, 50 µL of graded concentrations (50, 100 µg/mL) of LE-AgNPs and SE-AgNPs were added before incubation. Incubation conditions of 37°C for 24 hours and 27°C for 48 hours were employed for bacteria and fungi respectively. The zones of inhibition in millimeters were determined and the average for triplicate determinations were recorded.

Minimum Inhibitory concentration

The minimum inhibitory concentrations were determined by the addition of 2 mL of graded concentrations of LE-AgNPs to 18 mL of molten agar at 45°C to obtain final concentrations of 0.156, 0.312, 0.625, 1.25, 2.5, 5, 10 and 20 µg/mL. The mixture was thoroughly mixed before transferring to sterile petri dishes and allowed to set. A 0.5 McFarland standard suspension of overnight microbial culture were then spread on the surface of the agar and incubated. Incubation conditions of 37°C for 24 hours and 27°C for 48 hours were employed for bacteria and fungi respectively. After incubation, the plates were examined for microbial growth. The least concentrations of AgNPs that did not show microbial growth were recorded as the minimum inhibitory concentration. The MIC assay was similarly carried out for SE-AgNPs.

Determination of microbicidal concentration

The minimum microbicidal concentration was determined by swabbing the lowest concentrations of LE-AgNPs and SE-AgNPs that did not show microbial growth in the MIC assay on freshly prepared nutrient and Sabouraud dextrose agar plates. The concentrations of AgNPs that did not show microbial growth after incubation were recorded as the minimum microbicidal concentrations.

Catalytic degradation of methylene blue using as-synthesized AgNPs

The catalytic efficiency of the as-synthesized AgNPs was evaluated by UV-visible spectroscopic monitoring of the degradation of methylene blue in the presence of sodium borohydride. The optimized procedure with respect to concentrations of reagents is herein reported. In a conical flask, 10 mL of 0.01M

methylene blue solution and 2 mL of freshly prepared 0.2M NaBH₄ solution were diluted to 50 mL with distilled water before 5 mg of LE-AgNPs or SE-AgNPs was added. The UV-visible spectra of aliquots withdrawn from the reaction mixture after 5-minute intervals were then acquired. A blank reaction mixture that did not contain any nanocatalyst was also set up.

RESULTS AND DISCUSSION

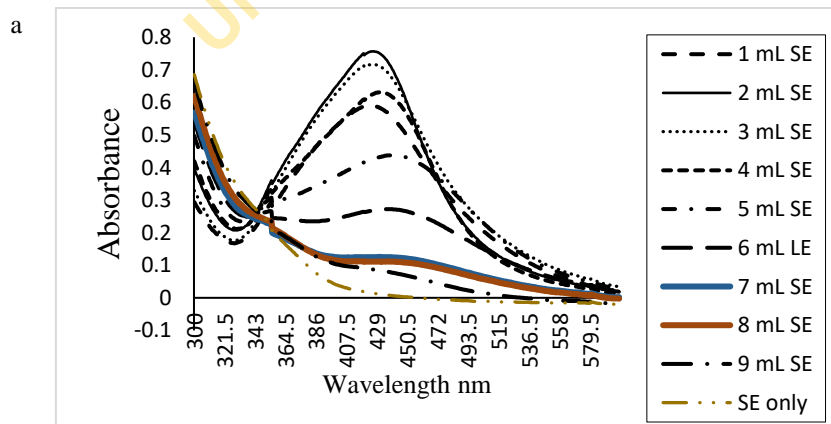
Phytoconstituents of *I. macrophylla*

Phytochemical analysis revealed the presence of tannins, terpenoids, phenols, alkaloids and steroids in both leaf and stem extracts. Phenolics, and hydroxylated constituents have been reported to be involved in the bioreduction of silver ions (Majoumou et al. 2019). In addition, analysis showed an abundance of flavonoids in the leaf extract.

UV spectroscopic monitoring of biosynthesis

The bioreduction of silver ions using the aqueous leaf extract was characterized by color change from greenish to yellowish brown solution as the LE-AgNPs were formed. Similarly, a color change to reddish brown was observed with the synthesis of SE-AgNPs. The color of colloidal solutions of AgNPs vary from yellow-green to blue depending on their particle size, morphology as well as the conditions of biosynthesis (Majoumou et al. 2019). The phytosynthesis of the AgNPs was therefore monitored with UV-vis spectroscopy. When AgNPs interact with

light of specific wavelengths, it causes the conduction electrons on the metal surface to undergo collective oscillation in a phenomenon known as surface plasmon resonance. This optical property of AgNPs is highly dependent on the nanoparticle diameter with smaller sized AgNPs exhibiting surface plasmon resonance at around 400 nm and larger particles at higher wavelengths up to 500nm (Paramelle et al. 2014). The UV-visible spectra of LE-AgNPs and SE-AgNPs exhibited plasmon resonance peaks at 430 and 426 nm respectively as shown in Fig. 1. This suggests that the particle sizes of LE-AgNPs and SE-AgNPs are both in the range of 60 nm (Paramelle et al. 2014). However, the aqueous leaf extract of *I. macrophylla* mediated the biosynthesis of AgNPs more rapidly and in greater yields than the stem extract. As shown in Fig. 1, extract-to-silver nitrate volume ratios of 10:90 and 20:80 were found optimal for biosynthesis using leaf and stem extracts respectively. An increase in volume ratio of stem extract not only led to less efficient production of nanoparticles (as indicated by lower absorption values) but also an increase in particle size as evidenced by the red shift in the spectra.



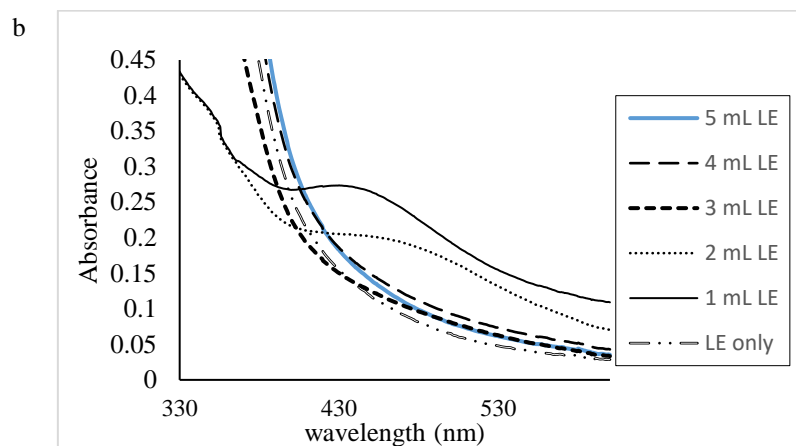


Figure 1. Spectral patterns of 10mL reaction mixtures containing varying volumes of (a) stem extract and (b) leaf extract

A 1mM solution of silver nitrate produced the highest yields of AgNPs as the use of more concentrated solutions led to progressive hypochromic changes in the spectral patterns of SE-AgNPs as shown in Fig. 2. A similar trend was observed with the biosynthesis of

LE-AgNPs as well as in other previous studies that have reported that the use of 1mM silver nitrate solution produced silver nanoparticles with improved yield and homogenous particle size (Ojha et al. 2013; Yusuf et al. 2020).

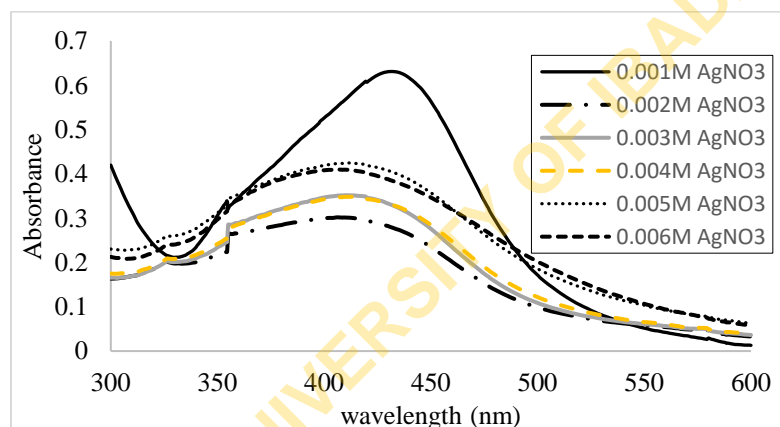


Figure 2. Variations in the spectral patterns of SE-AgNPs biosynthesized with different concentrations of AgNO_3

Characterization of biosynthesized AgNPs

FTIR identification of bioreductants

The bioreductants present in *I. macrophylla* that were involved in the synthesis and stabilization of LE-AgNPs and SE-AgNPs can be deduced from the FT-IR analysis of the nanoparticles. As depicted in Fig. 3, the vibrational frequencies found in the FT-IR spectra of SE-AgNPs included 3460 cm^{-1} , which corresponds to O-H stretch in alcohols and polyphenolic compounds including tannins. The observed vibrational frequency might also be due to the presence of amine salts. In addition, vibrational

frequencies at 2925.30 , 1640.44 and 1457.82 cm^{-1} that corresponds to C-Hstr, C=Cstr and C-H bending are most probably due to the involvement of hydrocarbons such as terpenoids which was found in abundance in the stem extract. The bands at 1640.44 and 1457.82 cm^{-1} may also be as a result of N-H and O-H bending in amine and alcohols or phenolics respectively. Thus, the biosynthesized SE-AgNPs were surrounded by phytochemicals including tannins, terpenoids and polyphenolics. These were able to serve as capping

agents and prevented the excessive agglomeration of the particles during synthesis. Very similar patterns were observed in the IR analysis of LE-AgNPs including the presence of a strong, sharp peak at 1641

cm^{-1} which has been attributed to the stretching vibrations of the C=O bonds of flavonoids (Yusuf et al. 2020)

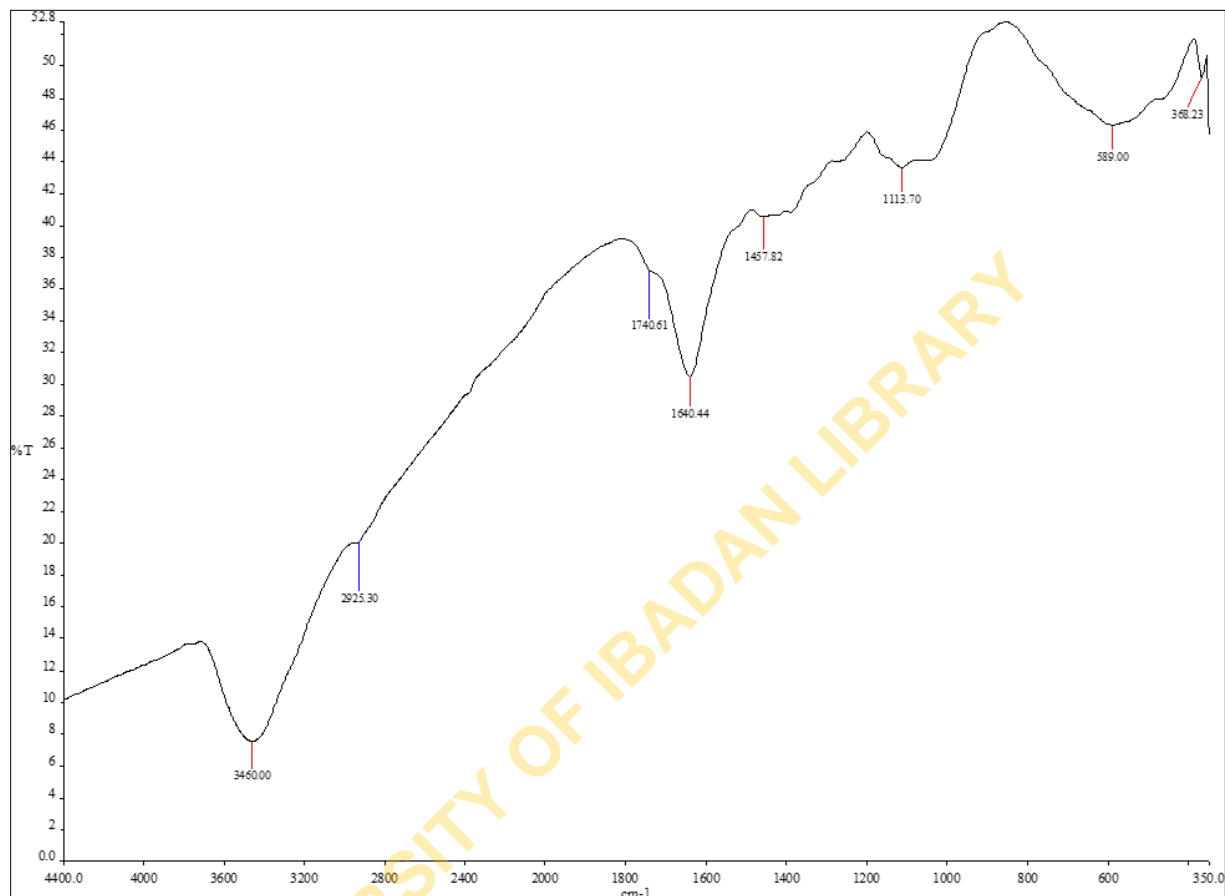


Figure 3. IR spectral patterns of SE-AgNPs

SEM and EDX Analyses

The SEM images were recorded from drop-coated films of the as-synthesized AgNPs. Fig. 4a depict the SEM image as well as the EDX analysis of the elemental composition of LE-AgNPs while Fig. 4b showed those of SE-AgNPs. The SEM images of LE-AgNPs and SE-AgNPs revealed highly aggregated polymorphs with mostly spherical or irregular shape. Similar results were obtained with the synthesis of AgNPs using *Cucumis prophetarum* (Hemlata et al.

2020). The EDX spectra of both LE-AgNPs and SE-AgNPs also showed an absorption band at 3KeV which is typical of metallic silver nanoparticles (Majoumou et al. 2019). The elemental analysis of the composition of LE-AgNPs and SE-AgNPs revealed a predominance of 75.46 and 73.66% silver respectively thus confirming the high efficiency of the aqueous leaf and stem extracts of *I. macrophylla* in the bioreduction of Ag^+ to Ag^0 .

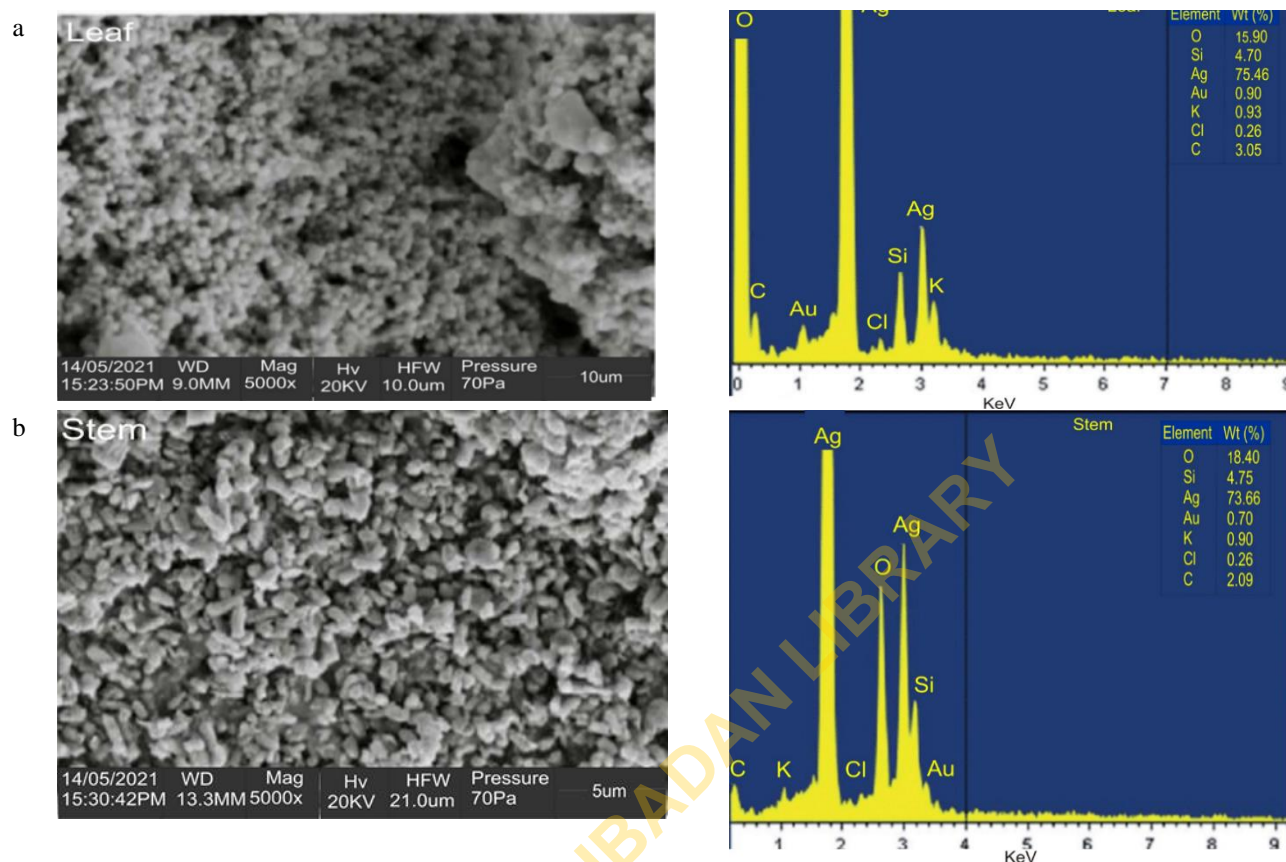


Figure 4. SEM-EDX Analyses of (a) LE-AgNPs and (b) SE-AgNPs

Morphology and particle size determination by TEM

The size and morphology of LE-AgNPs and SE-AgNPs were determined from TEM images as depicted in Fig. 5a and 5b respectively. TEM images showed that the nanoparticles were well separated with SE-AgNPs showing shapes that were more homogeneously spherical compared to LE-AgNPs that were mostly irregular in shape.

The mean particle size of LE-AgNPs and SE-AgNPs as determined by TEM were 48.61 ± 8.60 and 18.09 ± 4.13 nm respectively. Previous attempts to synthesize AgNPs using *Cucumis prophetarum*, *Terminalia mentaly* and *Clinacanthus nutans* produced nanoparticles with size distribution of 30-50, 11-83 and 10-180 nm respectively (Majoumou et al.

2019; Hemlata et al. 2020; Yusuf et al. 2020). In this study, we have therefore successfully synthesized small sized AgNPs with narrower size distribution. The size, size distribution and shape of metal nanoparticles are critical determinants of their biosensing, antimicrobial, catalytic and optic properties (Abou El-Nour et al. 2010; Rafique et al. 2017). In particular, small-sized quasi-shaped AgNPs exhibit superior catalytic efficiency (Sharma et al. 2015). Small sized AgNPs also show increased antimicrobial activity presumably due to their increased ability to cross cell wall of microorganisms (Abou El-Nour et al. 2010).

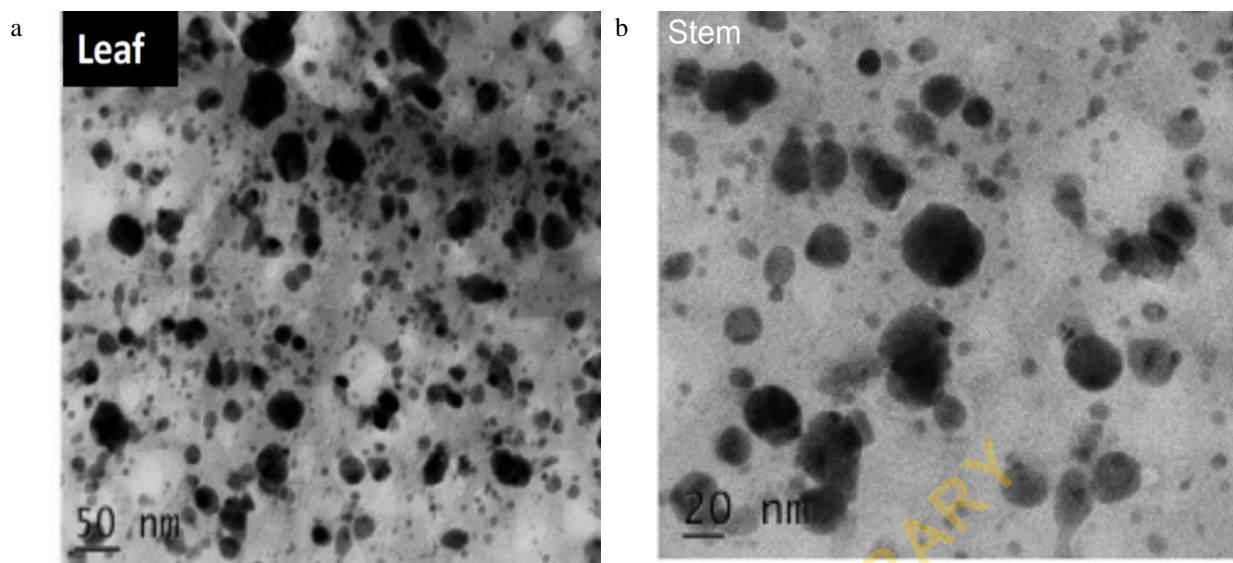


Figure 5. TEM images of (a) LE-AgNPs and (b) SE-AgNPs

Antimicrobial activities of biosynthesized AgNPs

Microbial susceptibility to as-synthesised AgNPs

Microorganisms are often used as indicator of water pollution with *E.coli* being the most commonly used faecal indicator. However, with increasing incidences of water-borne diseases from consumption of otherwise “safe” water, a number of nations such as the EU have defined additional indicator bacteria including *Staphylococci* and *Pseudomonas* species (Wen et al. 2020). We therefore assessed the antimicrobial activity of the biosynthesized AgNPs against these indicator bacteria among other species. The results as shown in Table 1 revealed that LE-AgNPs showed dose-dependent antimicrobial activity against *E. coli*, *Staphylococcus aureus* and *Pseudomonas aeruginosa*. In comparison, a narrower

spectrum of activity or decreased inhibitory activity at similar test concentrations were reported for AgNPs biosynthesized using *Datura metel* and *Thevetia peruviana* (Ojha et al. 2013; Oluwaniyi et al. 2016; Rafique et al. 2017). The results of the antimicrobial assay also revealed that LE-AgNPs and SE-AgNPs showed activity against the test organisms to varying extent. More pronouncedly, LE-AgNPs at concentrations of 50 and 100 $\mu\text{g/mL}$ inhibited the growth of both Gram positive and negative bacteria as well as fungi. On the other hand, SE-AgNPs only showed activity against *S. aureus* and *B. subtilis* at the highest test concentrations.

Table 1. Antimicrobial activity of silver nanoparticles biosynthesized using *I. macrophylla*

Test sample	Conc. ($\mu\text{g mL}^{-1}$)	Zone of inhibition (mm)					
		<i>S. aureus</i>	<i>B. subtilis</i>	<i>E. coli</i>	<i>P. aeruginosa</i>	<i>C. albicans</i>	<i>T. rubrum</i>
LE-AgNP	100	18	26	18	20	16	18
	50	16	20	14	16	14	14
SE-AgNP	100	10	10	0	0	0	0
	50	0	0	0	0	0	0
Gentamycin	10	20	22	18	18	NA	NA
Ketoconazole	10	NA	NA	NA	NA	22	20

NA-Not Applicable

The antibacterial activity of LE-AgNPs was similar to those obtained with silver nanoparticles biosynthesized using *Cucumis prophetarum* or *Garcinia kola* in which zones of inhibition of 14-18 and 17-20 mm were observed with Gram positive and

negative bacteria respectively (Labulo et al. 2016; Hemlata et al. 2020). In addition, *Candida albicans* was better inhibited by LE-AgNPs than with silver nanoparticles biosynthesized using *Garcinia kola* which showed zones of inhibition of 12 and 9 mm at

test concentrations of 125 and 62.5 µg/mL respectively (Labulo et al. 2016).

Thus, despite its relatively larger particle size, LE-AgNPs showed an enhanced antimicrobial activity compared to SE-AgNPs. The difference in activities might be due in part to the type of phytochemicals present on the nanoparticles. Phytochemical analysis revealed the abundance of flavonoids in the leaf extract which was completely absent in the stem. Flavonoids were subsequently identified by IR analysis as capping agents in LE-AgNPs. Biogenic nanoparticles with predefined characteristics can often be biosynthesized by use of plants with the desired biological activity in which case the bioactive phytoconstituents are present as capping agents on the AgNPs. It is widely reported that flavonoids and its hydroxylated forms including flavonols, flavones and flavanones show strong binding affinities to bacteria cell wall that compromise their growth and survival (Aires et al. 2016). Consequently, flavonoids-capped LE-AgNPs would be expected to show an enhanced antimicrobial activity. A similar additive effect was reported in the antimicrobial activity of antibiotic-capped AgNPs (Kora and Rastogi 2013).

It can also be observed from Table 1 that LE-AgNPs (at 50 and 100 µg/mL) showed higher activity against Gram-positive *S. aureus* and *B. subtilis* than the Gram-negative bacteria. Similarly, SE-AgNPs showed activity only against Gram-positive bacteria. This difference in susceptibility of Gram positive and negative organisms to antibacterial agents might be attributed to cell wall structure. Although, Gram-negative bacteria only have a single layer of peptidoglycan, they compensate for this with a cell

wall envelope that is made of three layers viz, an inner multifunctional membrane responsible for cellular biosynthetic functions, the middle single layer of peptidoglycan that confers rigidity and an outer protective membrane. Gram-negative bacteria are therefore often more resistant as antibiotics must pass through the protective membrane to reach their target sites in the bacteria (Breijyeh et al. 2020). The relatively small sizes of the biosynthesized nanoparticles will however, facilitate the penetration of the outer protective cell layer, followed by the disruption of cell membrane and cell death. Other mechanisms that have been proposed for the antimicrobial activity of AgNPs include ion-mediated killing in which silver ions released from colloidal AgNPs solutions combine with functional groups including thiol, carboxyl groups in the bacteria leading to the deactivation of several cellular functions and; contact killing in which AgNPs are immobilized on a suitable support (Agnihotri et al. 2013).

Minimum inhibitory and microbicidal concentrations

The minimum inhibitory and microbicidal concentrations of LE-AgNPs, which showed activity against the test organisms are depicted in Table 2. Fungi were less susceptible to the nanoparticles than bacteria. The mechanism for antifungal activity has been proposed to be due to the deactivation of sulfhydryl group on the organism cell wall followed by precipitation of insoluble cellular contents, disruption of membrane enzymes leading to cell lysis and death (Ajitha et al. 2015; Xia et al. 2016).

Table 2. Minimum Inhibitory and microbicidal concentrations of LE-AgNPs against test organisms

Test organisms	Minimum Inhibitory Concentration (µg mL ⁻¹)	Minimum Microbicidal Concentration (µg mL ⁻¹)
<i>S. aureus</i> ATCC 29213	5	10
<i>B. subtilis</i>	0.3125	0.3125
<i>E. coli</i> ATCC 25922	0.625	0.625
<i>P. aeruginosa</i> ATCC 27853	10	20
<i>C. albicans</i>	20	20
<i>T. rubrum</i>	20	20

Catalytic efficiency of as-synthesised AgNPs in degradation of methylene blue

Methylene blue is a basic aniline dye that is widely used in medicine as a marker dye and in the treatment of clinical conditions including urinary tract infections and methemoglobinemia (Smithson and Mitchell

2019). The dye loses its intense blue color as it degrades to the colorless leucomethylene blue in a reduction reaction that involves the acceptance of electrons from sodium borohydride. The catalytic

ability of the as-synthesized AgNPs to facilitate the electron transfer was therefore investigated by the periodic monitoring of the UV spectra of different reaction mixtures of methylene blue and sodium borohydride in the presence or absence of the AgNPs. Changes in the UV-vis spectra of reaction mixtures containing LE-AgNPs, SE-AgNPs and no

nanocatalyst are depicted in Fig. 6a, 6b and 6c respectively. In each case, the decrease in the absorbance of methylene blue at 664 nm offered good correlation with first order kinetics. Plots of relative absorbance as against time were generated and used to estimate first order rate constants for each of the reaction mixtures as shown in Figure 6d.

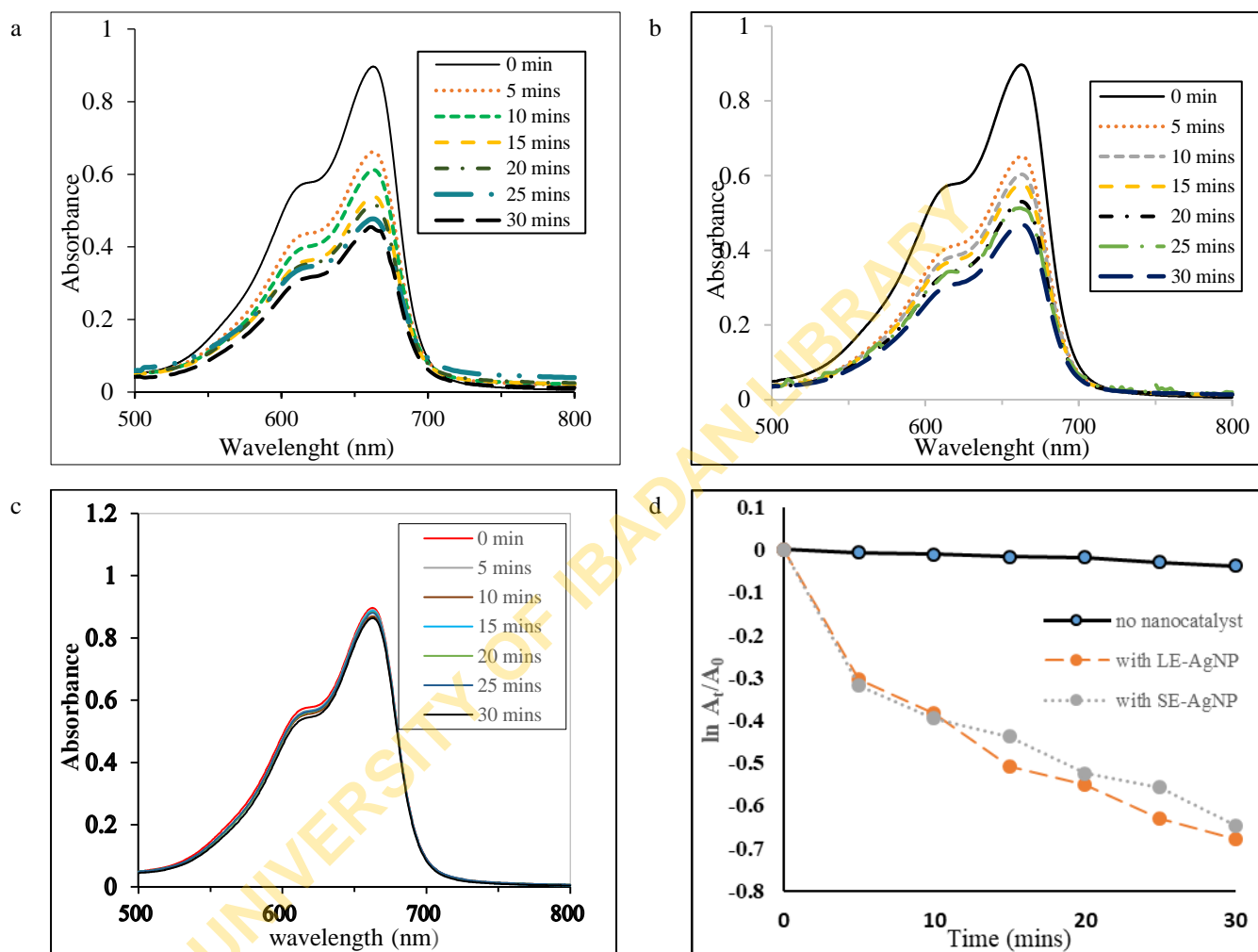


Figure 6. Reduction of methylene blue (a) with LE-AgNP (b) with SE- AgNP (c) without nanocatalyst (d) plots of A/A_0 against time

The rate constants for the degradation of methylene blue in the presence of LE-AgNPs and SE-AgNPs were 0.0204 and 0.0182 min^{-1} respectively compared to 0.0012 min^{-1} obtained in the absence of nanocatalyst. This represents a 17- and 15.6-fold increase in the rate of degradation of methylene blue with the inclusion of LE-AgNP and SE-AgNP respectively. The percent degradation of methylene blue after 30 minutes for LE-AgNP and SE-AgNP were 50.7 and 47.7% respectively, which were higher than 3.5% degradation observed in the absence of

nanocatalyst after the same period. The rate and extent of methylene blue degradation were therefore several folds greater than the uncatalysed reaction. When compared with other studies, AgNPs biosynthesized using *I. macrophylla* exhibited good catalytic efficiency as the rate constants of 0.0204 and 0.0182 min^{-1} were higher than 0.0014 min^{-1} obtained with silver nanoparticles biosynthesized using *Zanthoxylum armatum* (Jyoti and Singh 2016). The mechanism of catalysis by AgNPs involve an improvement in efficiency of the electron transfer

process from borohydride ions to the dye. This will in turn lead to a reduction of the bond dissociation energy that must be surmounted to destroy the aromatic stability of the dye. Irregularly shaped LE-AgNPs were found to be more efficient catalysts in this regard

compared to SE-AgNPs. This is in agreement with other studies that have found that quasi-spherical and irregularly shaped nanoparticles were more effective as catalysts (Sharma et al. 2015).

CONCLUSION

The green synthesis of silver nanoparticles using aqueous extracts of the leaf and stem of *Indigofera macrophylla* has been successfully achieved. The biosynthesized nanoparticles were capped with the plant's phytoconstituents. Quasi-spherical silver

nanoparticles obtained with the aqueous leaf extract exhibited superior antimicrobial and biocatalytic activities compared to nanoparticles biosynthesized using stem extract.

REFERENCES

- Abou El-Nour, K., Aftaiha, A., Al-Warthan, A., Amma, R. (2010). Synthesis and applications of silver nanoparticles. Arab. J. of Chem. 3: 135-140
- Adegoke, O.A., Ayodele, O.T. (2017). Novel Manganese Colorimetric Chemosensing Investigations of *Indigofera macrophylla* Schum (Thonn.) Stem and Leaf dye Extracts, Niger J Pharm Res 13:115-125.
- Agnihotri, S., Mukherji, S., Mukherji S. (2013). Immobilized silver nanoparticles enhance contact killing and show highest efficacy: elucidation of the mechanism of bactericidal action of silver, Nanoscale 5:7328–7340. <https://doi.org/10.1039/C3NR00024A>
- Aires, A., Marrinhas E., Carvalho R. (2016). Phytochemical Composition and Antibacterial Activity of Hydroalcoholic Extracts of *Pterospartum tridentatum* and *Mentha pulegium* against *Staphylococcus aureus* Isolates, Biomed Res Int 2016:5201879. <https://doi.org/10.1155/2016/5201879>
- Ajitha, B., Reddy, Y.A.K., Reddy, P.S. (2015). Biosynthesis of silver nanoparticles using *Momordica charantia* leaf broth: evaluation of their innate antimicrobial and catalytic activities, J Photochem Photobiol B Biol 146:1–9
- Al-Zaban, M.I., Mahmoud, M.A., AlHarbi, M.A. (2021). Catalytic degradation of methylene blue using silver nanoparticles synthesized by honey, Saudi J Biol Sci 28:2007–2013. <https://doi.org/10.1016/j.sjbs.2021.01.003>
- Breijyeh, Z., Jubeh, B., Karaman, R. (2020). Resistance of Gram-negative bacteria to current antibacterial agents and approaches to resolve it, Molecules 25:1340. <https://doi.org/10.3390/molecules25061340>
- Fierascu, R.C., Ortan, A., Avramescu, S.M., Fierascu, I. (2019). Phyto-Nanocatalysts: Green Synthesis, Characterization, and Applications, Molecules 24:3418
- Hemlata, Meena, P.R., Singh, A.P., Tejavath, K.K. (2020). Biosynthesis of silver nanoparticles using *cucumis prophetarum* aqueous leaf extract and their antibacterial and antiproliferative activity against cancer cell lines, ACS omega 5:5520–5528
- Jyoti, K., Singh, A. (2016). Green synthesis of nanostructured silver particles and their catalytic application in dye degradation, J Genet Eng Biotechnol 14:311–317. <https://doi.org/https://doi.org/10.1016/j.jgeb.2016.09.005>
- Kora, A.J., Rastogi, L. (2013). Enhancement of Antibacterial Activity of Capped Silver Nanoparticles in Combination with Antibiotics, on Model Gram-Negative and Gram-Positive Bacteria, Bioinorg Chem Appl 2013:871097. <https://doi.org/10.1155/2013/871097>
- Labulo, A.H., Adesuji, T.E., Oseghale, C.O., et al (2016). Biosynthesis of silver nanoparticles using *Garcinia kola* and its antimicrobial potential, African J Pure Appl Chem 10:1–7
- Majoumouo, M.S., Sibuyi, N.R.S., Tincho, M.B., et al (2019). Enhanced anti-bacterial activity of biogenic silver nanoparticles synthesized from *Terminalia mantaly* extracts, Int J Nanomedicine 14:9031–9046. <https://doi.org/10.2147/IJN.S223447>
- Menon, S., Agarwal, H., Shanmugam, V.K. (2021). Catalytical degradation of industrial dyes using biosynthesized selenium nanoparticles and evaluating its antimicrobial activities, Sustain Environ Res 31:2. <https://doi.org/10.1186/s42834-020-00072-6>
- Nwankwo, O.E., Ayodele, A.E. (2017). Taxonomic Studies of the Genus *Indigofera* Linn., in Nigeria, IDOSR J Sci Res 3:10–16
- Ojha, A.K., Rout, J., Behera, S., Nayak, P.L. (2013). Green synthesis and characterization of zero valent silver nanoparticles from the leaf extract of *Datura metel*, Int J Pharm Res Allied 2:31–35

- Oluwaniyi, O.O., Adegoke, H.I., Adesuji, E.T., et al (2016). Biosynthesis of silver nanoparticles using aqueous leaf extract of *Thevetia peruviana* Juss and its antimicrobial activities, *Appl Nanosci* 6:903–912
- Paramelle, D., Sadovoy, A., Gorelik, S., et al (2014). A rapid method to estimate the concentration of citrate capped silver nanoparticles from UV-visible light spectra, *Analyst* 139:4855–4861. <https://doi.org/10.1039/C4AN00978A>
- Rafique, M., Sadaf, I., Rafique, M.S., Tahir, M.B. (2017). A review on green synthesis of silver nanoparticles and their applications, *Artif cells, nanomedicine, Biotechnol* 45:1272–1291
- Renny, J., Tomasevich, L., Tallmadge, E., Collum, D. (2013). Method of continuous variations: Applications of Job plots to the study of molecular associations in organometallic chemistry, *Angew Chem Int Ed Engl* 52(46): 11998-12013
- Sharma, K., Singh, G., Kumar, M., Bhalla, V. (2015). Silver nanoparticles: Facile synthesis and their catalytic application for the degradation of dyes, *RSC Adv* 5:25781–25788. <https://doi.org/10.1039/c5ra02909k>
- Smithson, J., Mitchell, P.B. Antidepressants. In: *A Worldwide Yearly Survey of New Data in Adverse Drug Reactions*. Ed. Ray, S., Elsevier, Amsterdam 2019, 13–26
- Tripathi, R.M., Kumar, N., Shrivastav, A., et al (2013). Catalytic activity of biogenic silver nanoparticles synthesized by *Ficus panda* leaf extract, *Journal of Molecular Catalysis B : Enzymatic* 96:75–80
- Wen, X., Chen, F., Lin, Y., et al (2020). Microbial indicators and their use for monitoring drinking water quality—a review, *Sustainability* 12:2249
- Xia, Z-K, Ma, Q-H, Li, S-Y, et al (2016). The antifungal effect of silver nanoparticles on *Trichosporon asahii*, *J Microbiol Immunol Infect* 49:182–188. <https://doi.org/https://doi.org/10.1016/j.jmii.2014.04.013>
- Yusuf, S.N., Mood, C.N., Ahmad, N.H., et al (2020). Optimization of biogenic synthesis of silver nanoparticles from flavonoid- rich *Clinacanthus nutans* leaf and stem aqueous extracts, *R Soc Open Sci* 7:200065. <https://doi.org/http://dx.doi.org/10.1098/rsos.200065>

*Address for correspondence: Olusegun E. Thomas
Department of Pharmaceutical Chemistry,
Faculty of Pharmacy,
University of Ibadan,
Nigeria.
Telephone: +2348034198737
E-mails: seguntom@yahoo.com

Conflict of Interest: None declared

Received: March 08, 2022

Accepted: May 06, 2022